Published in final edited form as:
J Hepatol. 2011 May ; 54(5): 994–1001. doi:10.1016/j.jhep.2010.08.034.

OVEREXPRESSION OF THE IGF2-mRNA BINDING PROTEIN *p62* IN TRANSGENIC MICE INDUCES A STEATOTIC PHENOTYPE

Elisabeth Tybl[1], **Fu-Dong Shi**[2], **Sonja M. Kessler**[1], **Sascha Tierling**[3], **Jörn Walter**[3], **Rainer M. Bohle**[4], **Stefan Wieland**[5], **Jianying Zhang**[6], **Eng M. Tan**[5], and **Alexandra K. Kiemer**[1,*]

[1]Saarland University, Department of Pharmacy, Pharmaceutical Biology, Saarbrücken, Germany

[2]Barrow Neurological Institute, St. Joseph´ s Hospital and Medical Center, Phoenix, USA

[3]Saarland University, Institute of Genetics/Epigenetics, Saarbrücken, Germany

[4]Department of Pathology, Saarland University, Homburg/Saar, Germany

[5]The Scripps Research Institute, Department of Molecular and Experimental Medicine, La Jolla, USA

[6]University of Texas El Paso, Department of Biology, El Paso, Texas, USA

Abstract

Background & Aims—The insulin-like growth-factor 2 (*IGF2*) mRNA binding protein *p62* is highly expressed in hepatocellular carcinoma tissue. Still, its potential role in liver disease is largely unknown. In this study we investigated pathophysiological implications of *p62* overexpression in mice.

Methods—We generated mice overexpressing *p62* under an LAP-promotor. mRNA expression levels and stability were examined by real-time RT-PCR. Allele-specific expression of *Igf2* and *H19* were assessed after crossing mice with SD7 animals. The *Igf2* downstream mediators pAKT and PTEN were determined by Western Blot.

Results—Hepatic *p62* overexpression did neither induce inflammatory processes or liver damage. However, 2.5 week old transgenic animals displayed a steatotic phenotype and improved glucose tolerance. *p62* overexpression induced the expression of the imprinted genes *Igf2* and *H19* and their transcriptional regulator Aire (autoimmune regulator). Neither monoallelic expression nor mRNA stability of *Igf2* and *H19* was affected. Investigating *Igf2* downstream signalling pathways showed increased AKT activation and attenuated PTEN expression.

Conclusion—The induction of a steatotic phenotype implies that *p62* plays a role in hepatic pathophysiology.

*To whom correspondence should be addressed, Alexandra K. Kiemer, Ph.D., Saarland University, P.O. box 15 11 50, 66041 Saarbrücken, Germany, phone: +49-681-302 57301, fax: +49-681-302 57302, pharm.bio.kiemer@mx.uni-saarland.de.

E. Tybl, S.M. Kessler, and A.K. Kiemer designed experiments, analysed data and wrote the manuscript. A.K. Kiemer and E.M. Tan initiated and directed the study. The others generated *p62* transgenic mice, designed experiments, and participated in data acquisition. There are no conflicts of interest to disclose.

Keywords

PTEN; IMP; NAFLD; NASH; CMV promoter activity; p65

Introduction

During the past 20 years a rise in HCC incidence has been noticed, which is associated with metabolic risk factors like obesity, diabetes mellitus, non-alcoholic fatty liver disease (NAFLD), and non-alcoholic steatohepatitis (NASH) [1].

The oncofetal protein *p62* was originally identified as a 62 kDa autoantigen from a patient suffering from HCC [2]. *p62* belongs to the family of *IGF2* mRNA-binding proteins (IMPs) and represents a splice variant of IMP2. *p62* expression is absent in adult livers, but can be found in HCC nodules and in fetal liver [3]. IMPs have been shown to be implicated in growth promotion, carcinogenesis, and tumor progression [4–6]. The interaction of *p62* and *IGF2* might be of special interest with regard to the tumor-promoting nature of IGF2: reduced IGF2 expression was shown to enhance survival from HCC [7], and a dysregulation of the haploidic imprinting status of *IGF2* and *H19* is associated with metabolic diseases and cancer development [8].

IGF2 plays a key role in mammalian growth through metabolic and growth-promoting effects [9]. The induction of downstream signal transduction pathways is mediated mainly through the activation of phosphoinositide 3 (PI3)-kinase/AKT [10] and AKT inactivation is facilitated by the tumor-suppressor PTEN (phosphatase and tensin homolog [10,11].

Since a potential role of *p62* in liver disease is largely unknown, we characterized a mouse model in which *p62* was exclusively overexpressed in the liver. The animals developped fatty livers at an early age, paralleled by a non-inflammatory phenotype.

Materials and Methods

Animals

All animal procedures were performed in accordance with the local animal welfare committee.

The targeting vector contained the human *p62* protein under control of the transrepressive responsive element cytomegaly virus (TRE-CMV_{min}) promotor (Fig. 1A). In order to induce *p62* expression, transgenic mice were bred with LT2 mice, which carry a liver enriched activator protein (LAP) under control of a tetracycline transactivator (tTA) [12]. Liver-specific expression of the transgene can be switched off by the application of doxycycline (Fig. 1A).

$p62^{+}$/$LT2^{+}$ (*p62*) were compared to $p62^{-}$/$LT2^{+}$ (co) in all experiments. Primer sequences for genotyping are given in supplementary data.

After microinjection, two mouse lineages founded on a different background were maintained. In lineage 23, only males displayed the transgene. If not stated otherwise, experiments were performed on lineage 50 to consider gender-specific differences.

p62/SD7 mice

LT2 mice were bred to homozygous SD7 animals to produce reciprocal F2 progeny (LT2 × *Mus spretus*) [13]. 2.5 week old $p62^{+}$/$LT2^{+}$ and $p62^{-}$/$LT2^{+}$ mice being heterozygous for the *Mus spretus* allele were analysed.

Real-time quantitative polymerase chain reaction

Experiments and quantification were performed as described in detail in [14,15]. Sequences and conditions are given in supplementary data.

Allele-specific expression analysis using single-nucleotide primer extension (SNuPE)

Primer extension was performed employing SNuPE primers placed adjacent to the polymorphic sites. All steps are described in detail in [16]. The allele-specific expression index was assessed by calculating the ratio h(C)/[h(C)+h(T)].

IP-Glucose Tolerance Test (IP-GTT)

2.5 week old mice were starved before they were given a single i. p. injection (10 µl/g body weight) of glucose (B. Braun, Melsungen, Germany). Circulating glucose levels were measured with an Accu-Check Aviva glucometer (Roche Diagnostics, Mannheim, Germany).

Serum analysis

2.5 week old mice were starved and sacrificed. Serum levels were determined at the “Zentrallabor des Universitätsklinikums des Saarlandes” (Homburg, Germany).

Hepatocyte isolation and mRNA stability

Hepatocytes were isolated using a modified two-step collagenase perfusion method [17] with a viability exceeding 80 %.

Cells were cultured on collagen-coated plates and the next day treated with 10 µg/ml ActD at different time points [18] (see supplementary data).

Histology and immunohistology

Staining was performed either on cryosections or paraffin-embedded tissues. Detection for immunohistochemistry was done with the CSA II kit (DAKO, Hamburg, Germany).

Western blot analysis

Western blots were performed according to [19]. Antibodies used were specific to phosphoAKT (Ser473), PTEN (New England Biolabs, Frankfurt a. M., Germany and α-tubulin (Sigma, Thermo Fisher Scientific, Karlsruhe, Germany).

Statistical analysis

Groups were compared using student´ s t-test for independent, normally distributed samples. Data represent the mean ± standard error of the mean (SEM). P values less than .05 were considered significant.

Results

Liver specific expression of *p62*

Solely double-positive ($p62^{+}$/$LT2^{+}$) mice expressed the transgene in the liver (Fig. 1A+B). Doxycyclin administration abrogated *p62* expression (Fig. 1C). Expression levels of *p62*

showed rather high interindividual variability and strongly decreased at the age of 10 weeks (Fig. 1D) although LAP activity increased with age, as shown by increased tTA expression in $LT2^+$ mice (Fig. 1E). *p62* expression is restricted to the cytoplasm (Fig. 1F).

Induction of a fatty liver in 2.5 week old *p62* transgenic mice

Livers displayed an accumulation of basophilic cells around the central veins (Rappaport zone 1, Fig. 2A). Leukocyte infiltration was not observed.

A decrease in glycogen staining indicated metabolic alterations (Fig. 2B).

Liver architecture gave hints of an accumulation of neutral lipids. Specific fat staining demonstrated a steatotic phenotype with a significant rise in fat droplets without a preferred zonal distribution in 58% of animals (Fig. 2C). Fatty livers occurred with a higher frequency in females (66%) when compared to males (44%).

Livers of animals at older age displayed no histological alterations.

p62 transgenic animals at 2.5 and 5 weeks of age displayed a non-significant difference in liver weight, with a tendency towards lower body weights. A slight but significant increase in the liver to body weight ratio was only observed at the age of 2.5 weeks (Fig. 3A). Serum cholesterol and HDLC did not differ, neither with regard to gender nor the experimental groups (Fig. 3B). However, a slight but significant increase in triglyceride (TG) levels was found in males (Fig. 3B).

Absence of liver damage and inflammation

In order to determine characteristics of NASH, i.e. liver alterations encompassing inflammation, a potential activation/translocation of NF- κB (p65 subunit), which plays a pivotal role in the inflammatory response, was determined.

Nuclear p65 in immune cells, indicating inflammatory activity, was detected to a very low extent in both experimental groups (Fig. 3C). Interestingly, however, an increased cytoplasmic staining of hepatocytes was revealed in 80% of transgenic animals compared to controls.

The lack of an increase in serum transaminases underlined the absence of inflammation (Fig. 3B).

Increased expression of *Igf2* and *H19*

Since *p62* belongs to the family of *IGF2* mRNA-binding proteins and due to the fact that *IGF2* shares an imprinting control region with *H19* [20], potential expression changes were determined.

A significant upregulation of *Igf2* and *H19* could be shown (Fig. 4A). This effect of *p62* overexpression on *Igf2* and *H19* was not due to genetic predisposition: after administration of doxycycline, *Igf2* and *H19* levels declined, also seen in another lineage (Fig. 4B and supplementary Fig. 1). *p62* transgenic females displayed higher *Igf2* and *H19* mRNA expression levels in comparison to males, further supported by the detection of a lower *p62* expression in another lineage, where only males express the transgene (Fig. 4B and supplementary Fig. 1). When we grouped 2.5 week old animals into fatty liver and non-fatty liver transgenic mice neither differences in *p62* nor *H19* expression were observed (Fig. 4C). However, *Igf2* levels were higher in fatty livers than in phenotypically normal transgenic tissues (Fig. 4C).

Mechanisms of *Igf2* and *H19* induction

With *p62* being an mRNA binding protein it might regulate mRNA stability [21]. *Igf2* and *H19* mRNA stability was estimated in actinomycin D-treated hepatocytes. Fig. 5A shows that steady-state levels of all mRNAs decreased similarly over time and more than 50 % of mRNA levels were left after 10 h.

Since no stabilizing action of *p62* on *Igf2* and *H19* mRNA was observed, we investigated allele-specific expression of *Igf2* and *H19*. A mono-allelic *Igf2* and *H19* expression could be demonstrated in both groups (Fig. 5B), corresponding to an allele-specific index of 1.0.

Both *Igf2* and *H19* have been reported to be strongly induced by the transcriptional regulator Aire (autoimmune regulator) [22]. Interestingly, Aire expression was significantly increased in *p62* transgenic animals at the age of 2.5 and 5 weeks, whereas it was downregulated at the age of 10 weeks (Fig. 5C). Female animals showed a slightly higher expression of Aire.

Activation of IGF2 downstream targets

Enhanced AKT phosphorylation at Ser473 was observed at the age of 5 and 10 weeks, whereas 2.5 week old animals showed no changes (Fig. 6A). A reduction of both PTEN protein and mRNA levels could be demonstrated for 2.5 and 10 week old *p62* transgenic mice (Fig. 6B/C).

Improved glucose tolerance

Since histological analyses suggested metabolic changes, an intraperitoneal glucose tolerance test (IP-GTT) was performed.

Fasting levels of glucose and end point values corresponded in both experimental groups. The time course revealed a slightly improved glucose clearance of *p62* transgenic animals at 30 min after glucose administration ($p>.05$) (Fig. 7A).

The glucose tolerance distribution curve in female *p62* transgenic mice revealed a significant reduction of glucose levels at 30 min (69.5 ± 10.8 %) and at 75 min (75.2 ± 15.1%) ($p <.05$, both) in comparison to controls. Differences in glucose tolerance were further supported by a significant decrease in the AUC (area under the curve: glucose concentration over time) of females only (Fig. 7B). In summary, the results indicate a gender-specifically enhanced glucose clearance in the presence of *p62*.

Discussion

The exclusive expression of *p62* in HCC cancer nodules [2] together with its appearance in fetal liver make it an oncofetal protein [3]. Functional implications of the protein have as yet been completely unknown. We herein present the first phenotypic characterization of liver-specific *p62* overexpression in transgenic mice.

Although no evidence of spontanous tumor formation upon *p62* overexpression was detected, a hint on an impact of *p62* on cell malignancy was given by HE-staining due to the appearance of basophilic cell foci in *p62* transgenic liver tissue, a phenotype suggesting a progressive cellular dedifferentiation [23].

Histological fat staining revealed the phenotype of a fatty liver with a microvesicular fat distribution in *p62* transgenic mice, as found in other genetic mouse models and in cases of human NAFLD [24]. Interestingly, fat accumulation was accompanied by increased *Igf2* expression, as also found in human fatty livers [25].

A steatotic phenotype is considered to be benign with little risk of disease progression unless inflammation is detected [26]. The lack of an increase in serum transaminases was also observed in dietary models of fatty livers [27]. Higher TG (triglyceride) levels as observed in male *p62* transgenic mice are not toxic *per se* and were also found in mice with a liver-specific nuclear respiratory factor 1 deletion [28] and the significant increase of the ratio of the liver to body weight is consistent with observations made in fatty liver models [29].

The decrease of glycogen in *p62* transgenic animals might represent an early stage of liver dysfunction, as it has been described in humans with alcohol-induced liver cirrhosis [30].

Since fatty livers are often connected to the establishment of insulin resistance leading to impaired glucose tolerance, IP-GTT was performed. A significant decrease in the area under the curve (AUC) in *p62* transgenic females could be demonstrated, indicating an increased ability to clear glucose. This observation is in concordance with improved glucose tolerance after liver-specific PTEN deletion in mice [24]. Interestingly, the effect of decreased PTEN is less pronounced at 5 weeks compared to 2.5 weeks of age, when actual fat depositions occur. This suggests PTEN downregulation as a critical feature in *p62*-induced steatosis.

The increase of pAKT, being known as a promotor of cell malignancy and a metabolic regulator [31], can be explained by *p62*-mediated *Igf2* induction. Also PTEN downregulation might support the increase in pAKT *via* the attenuated ability of PTEN to dephosphorylate the AKT activator PIP-3 [10]. Since AKT phosphorylation was not increased at the age when steatosis occurred, however, its pathophysiological role is suggested to be of minor relevance.

The gender differences in liver phenotypes reflect the observation that females express higher *Igf2* levels although *p62* levels were similar in males and females. Interestingly, the transcriptional regulator of *Igf2*, Aire [22] is also higher expressed in transgenic females and it is known to act gender-specifically [32]. Both fatty livers and improved glucose tolerance were more pronounced in females, suggesting a causal interaction between Aire-induced *Igf2* and the metabolic phenotype.

The shared regulation of *IGF2* and PTEN has been shown in several cancer cells [33] and a direct inhibition of PTEN expression by *Igf2* has been reported [34]. The *p62*-induced downregulation of PTEN might contribute to the increase in fatty acids as shown in mice with a liver-specific PTEN deletion [24]. *Vice versa* since fatty acids are able to downregulate PTEN [35], they might contribute to further declined PTEN expression.

The question whether the fatty liver phenotype in *p62* transgenic animals is accompanied by NASH, i. e. the additional occurrence of inflammation, was addressed by different approaches. No leukocyte infiltrates could be detected. The lack of transaminase increases, also observed in a genetic mouse model of NAFLD [28], as well as the absence of NF-κB translocation confirmed the absence of a pro-inflammatory phenotype. Interestingly, *p62* transgenic animals showed a distinct increase in cytosolic p65. Very few studies address changes in the expression levels of non-activated, i.e. cytosolic p65 [36], but an association with tumor diseases has been demonstrated in malignant epithelial cells from colorectal tissue [37]. Constitutive overexpression of the p65 protein has also been shown in thyroid carcinoma cells [38] and the oncogene MDM2 induces p65 protein expression in acute lymphoblastic leukemia [39]. Although functional implications of increased levels of p65 are as yet largely unknown, they might enhance an inflammatory response upon respective stimuli [36]. Whereas the microvesicular fat distribution in *p62* transgenic mice forms the borderline from a benign to a morbid condition [40], our results suggest that the “second hit” towards the progression of NASH, resulting from inflammation, is missing.

Our data report that *p62* induces both *IGF2* and *H19* [41] expression, which are known to play opposite roles in tumor development. Despite strongly increased *Igf2* levels, our animals did not develop tumors. This might be connected to high levels of the tumor suppressor gene *H19* [13]. Also the decline of transgene expression at the age of 10 weeks most likely contributes to the lack of the development of a malignant disease. Our data do not indicate that LAP-induced gene expression is downregulated with age, which is why we suggest that CMV promoter activity declines.

Since *p62* is a member of the IMP family [3] and IMPs have been reported to bind to *H19* [42], IMPs are potential candidates to influence mRNA stability [21]. However, our results revealed no influence of *p62* on mRNA stability of *Igf2* and *H19*. Since both mRNAs turned out to be rather stable mRNAs ($t_{1/2}$>10 h) the regulation *via* stabilizing mechanisms is rather unlikely since stability-regulated genes mostly represent short-lived mRNAs [21].

The counter-regulatory actions between *IGF2* and *H19* are very complex [43]. The imprinted genes *IGF2* and *H19* often show coordinate, reciprocal regulation [44,45]. On the other hand, Li et al. found parallel expression of *IGF2* and *H19* in HCC [46] and loss of imprinting (LOI) of *IGF2* in HCC has been associated with coexpression of *H19* and *IGF2* [47]. Therefore, investigations of the chromosomal expression of IGF2 and *H19* evoked by *p62* were done. However, neither a change in allele-specific nor biallelic expression was detected for *Igf2* and *H19*. Our result that LOI of the *IGF2* locus is not involved in increased *Igf2* gene expression in *p62* transgenic mice is in concordance with the observation made by Feinberg et al. [48].

The increased expression of the transcriptional regulator Aire is most likely responsible for the high expression of both *Igf2* and *H19* in *p62* transgenic animals: both *Igf2* and *H19* are among the genes most highly regulated by Aire expression [22]. Although Aire has been described to be found in hepatocytes to a high extent [49], a functional implication of Aire expression in the liver has as yet been completely unknown. Therefore, further studies need to establish an insight into the connection between the autoantigen *p62* and Aire, the latter being known to be an important regulator of autoimmunity [49].

Taken together, our data provide evidence that *p62* exhibits a distinct upregulation of the metabolic growth factor *Igf2 via* induction of the transcriptional activator Aire. *p62* seems to play a pathophysiological role in liver disease through its induction of a fatty liver phenotype. *p62* might therefore serve both as a diagnostic marker as well as a pharmacological target.

Supplementary Material

Refer to Web version on PubMed Central for supplementary material.

Acknowledgments

We thank Nikolaus Gladel, Marga Sand-Hill, Sieglinde Wagner, Gertrud Walter, and Daorong Liu for excellent technical assistance. We thank the Kistner group for providing LT2 mice. We are especially indebted to Dr. Frank Chisari of The Scripps Research Institute for his help and advice with induction of the *p62* transgenic mice.

The project was funded by the Deutsche Krebshilfe (#107751) and by grant CA 56956 from the National Institutes of Health, U.S.A. A.K.K. was supported by the Alexander von Humboldt foundation.

References

1. Takamatsu S, Noguchi N, Kudoh A, Nakamura N, Kawamura T, Teramoto K, et al. Influence of risk factors for metabolic syndrome and non-alcoholic fatty liver disease on the progression and

prognosis of hepatocellular carcinoma. Hepatogastroenterology. 2008; 55:609–614. [PubMed: 18613418]

2. Zhang JY, Chan EK, Peng XX, Tan EM. A novel cytoplasmic protein with RNA-binding motifs is an autoantigen in human hepatocellular carcinoma. J Exp Med. 1999; 189:1101–1110. [PubMed: 10190901]
3. Lu M, Nakamura RM, Dent ED, Zhang J-Y, Nielsen FC, Christiansen J, et al. Aberrant Expression of Fetal RNA-Binding Protein p62 in Liver Cancer and Liver Cirrhosis. Am J Pathol. 2001; 159:945–953. [PubMed: 11549587]
4. Jeng YM, Chang CC, Hu FC, Chou HY, Kao HL, Wang TH, Hsu HC. RNA-binding protein insulin-like growth factor II mRNA-binding protein 3 expression promotes tumor invasion and predicts early recurrence and poor prognosis in hepatocellular carcinoma. Hepatology. 2008; 48:1118–1127. [PubMed: 18802962]
5. Hansen TV, Hammer NA, Nielsen J, Madsen M, Dalbaeck C, Wewer UM, et al. Dwarfism and impaired gut development in insulin-like growth factor II mRNA-binding protein 1-deficient mice. Mol Cell Biol. 2004; 24:4448–4464. [PubMed: 15121863]
6. Hutchinson L. Medical oncology: IMP3 is a novel prognostic marker for colon cancer. Nat Rev Clin Oncol. 7:123.
7. Yao X, Hu JF, Daniels M, Shiran H, Zhou X, Yan H, et al. A methylated oligonucleotide inhibtis IGF2 expression and enhances survival in a model of hepatocellaular carcinoma. J Clin Invest. 2003; 111:265–273. [PubMed: 12531883]
8. Saho WJ, Tao LY, Gao C, Xie JY, Zhao RQ. Alterations in methylation and expression levels of imprinted genes H19 and Igf2 in the fetuses of diabetic mice. Comp Med. 2008; 58:341–346. [PubMed: 18724775]
9. Nielsen FC. The molecular and cellular biology of insulin-like growth factor II. Prog Growth Factor Res. 1992; 4:257–290. [PubMed: 1307492]
10. Suzuki A, Nakano T, Mak TW, Sasaki T. Portrait of PTEN: Messages from mutant mice. Cancer Science. 2008; 99:209–213. [PubMed: 18201277]
11. Vinciguerra M, Sgroi A, Veyrat-Durebex C, Rubbia-Brandt L, Buhler LH, Foti M. Unsaturated fatty acids inhibit the expression of tumor suppressor phosphatase and tensin homolog (PTEN) via microRNA-21 up-regulation in hepatocytes. Hepatology. 2009; 49:1176–1184. [PubMed: 19072831]
12. Kistner A, Gossen M, Zimmermann F, Jerecic J, Ullmer C, Lubbert H, Bujard H. Doxycycline-mediated quantitative and tissue-specific control of gene expression in transgenic mice. Proc Natl Acad Sci USA. 1996; 93:10933–10938. [PubMed: 8855286]
13. Yoshimizu T, Miroglio A, Ripoche MA, Gabory A, Vernucci M, Riccio A, et al. The H19 locus acts in vivo as a tumor suppressor. Proc Natl Acad Sci USA. 2008; 105:12417–12422. [PubMed: 18719115]
14. Kiemer AK, Senaratne RH, Hoppstädter J, Diesel B, Riley L, Tabeta K, et al. Attenuated activation of macrophage TLR9 by DNA from virulent mycobacteria. J Innate Immun. 2009; 1:29–45. [PubMed: 20375564]
15. Bouayed J, Desor F, Rammal H, Kiemer AK, Tybl E, Schroeder H, et al. Effects of lactational exposure to benzo[alpha]pyrene (B[alpha]P) on postnatal neurodevelopment, neuronal receptor gene expression and behaviour in mice. Toxicology. 2009; 259:97–106. [PubMed: 19428949]
16. Tierling S, Dalbert S, Schoppenhorst S, Tsai CE, Oliger S, Ferguson-Smith AC, et al. High-resolution map and imprinting analysis of the Gtl2-Dnchc1 domain on mouse chromosome 12. Genomics. 2006; 87:225–235. [PubMed: 16309881]
17. Kulhanek-Heinze S, Gerbes A, Gerwig T, Vollmar AM, Kiemer AK. Protein kinase A dependent signalling mediates anti-apoptotic effects of the atrial natriuretic peptide in ischemic livers. J Hepatol. 2004; 41:414–420. [PubMed: 15336444]
18. Kiemer AK, Vollmar AM. Autocrine Regulation of Inducible Nitric-oxide Synthase in Macrophages by Atrial Natriuretic Peptide. J Biol Chem. 1998; 273:13444–13451. [PubMed: 9593677]

19. Duenschede F, Tybl E, Kiemer AK, Dutkowski P, Erbes K, Kircher A, et al. Bcl-2 upregulation after 3-nitropropionic acid preconditioning in warm rat liver ischemia. Shock. 2008; 30:699–704. [PubMed: 18461020]
20. Sasaki H, Ishihara K, Kato R. Mechanisms of Igf2/H19 imprinting: DNA methylation, chromatin and long-distance gene regulation. J Biochem. 2000; 127:711–715. [PubMed: 10788777]
21. Eberhardt W, Doller A, Akool E-S, Pfeilschifter J. Modulation of mRNA stability as a novel therapeutic approach. Pharmacology & Therapeutics. 2007; 114:56–73. [PubMed: 17320967]
22. Johnnidis JB, Venanzi ES, Taxman DJ, Ting JPY, Benoist CO, Mathis DJ. Chromosomal clustering of genes controlled by the aire transcription factor. Proc Natl Acad Sci USA. 2005; 102:7233–7238. [PubMed: 15883360]
23. Su Q, Benner A, Hofmann WJ, Otto G, Pichlmayr R, Bannasch P. Human hepatic preneoplasia: phenotypes and proliferation kinetics of foci and nodules of altered hepatocytes and their relationship to liver cell dysplasia. Virchows Arch. 1997; 431:391–406. [PubMed: 9428927]
24. Stiles B, Wang Y, Stahl A, Bassilian S, Lee WP, Kim YJ, et al. Liver-specific deletion of negative regulator Pten results in fatty liver and insulin hypersensitivity. Proc Natl Acad Sci USA. 2004; 101:2082–2087. [PubMed: 14769918]
25. Chiappini F, Barrier A, Saffroy R, Domart MC, Dagues N, Azoulay D, et al. Exploration of global gene expression in human liver steatosis by high-density oligonucleotide microarray. Lab Invest. 2006; 86:154–165. [PubMed: 16344856]
26. Teli MR, James OF, Burt AD, Bennett MK, Day CP. The natural history of nonalcoholic fatty liver: a follow-up study. Hepatology. 1995; 22:1714–1719. [PubMed: 7489979]
27. Lee L, Alloosh M, Saxena R, Alstine Wv, Watkins BA, Klaunig JE, et al. Nutritional model of steatohepatitis and metabolic syndrome in the Ossabaw miniature swine. Hepatology. 2009; 50:56–67. [PubMed: 19434740]
28. Xu Z, Chen L, Leung L, Yen TS, Lee C, Chan JY. Liver-specific inactivation of the Nrf1 gene in adult mouse leads to nonalcoholic steatohepatitis and hepatic neoplasia. Proc Natl Acad Sci USA. 2005; 102:4120–4125. [PubMed: 15738389]
29. Otogawa K, Kinoshita K, Fujii H, Sakabe M, Shiga R, Nakatani K, et al. Erythrophagocytosis by liver macrophages (Kupffer cells) promotes oxidative stress, inflammation, and fibrosis in a rabbit model of steatohepatitis: implications for the pathogenesis of human nonalcoholic steatohepatitis. Am J Pathol. 2007; 170:967–980. [PubMed: 17322381]
30. Owen OE, Reichle FA, Mozzoli MA, Kreulen T, Patel MS, Elfenbein IB, et al. Hepatic, gut, and renal substrate flux rates in patients with hepatic cirrhosis. J Clin Invest. 1981; 68:240–252. [PubMed: 7251861]
31. O´Connor R. Survival factors and apoptosis. Adv Biochem Eng Biotechnol. 1998; 62:137–166. [PubMed: 9755644]
32. Hassler S, Ramsey C, Karlsson MC, Larsson D, Herrmann B, Rozell B, et al. Aire-deficient mice develop hematopoetic irregularities and marginal zone B-cell lymphoma. Blood. 2006; 108:1941–1948. [PubMed: 16709926]
33. Perks CM, Vernon EG, Rosendahl AH, Tonge D, Holly JM. IGF-II and IGFBP-2 differentially regulate PTEN in human breast cancer cells. Oncogene. 2007; 26:5966–5972. [PubMed: 17369847]
34. Moorehead RA, Hojilla CV, De Belle I, Wood GA, Fata JE, Adamson ED, et al. Insulin-like growth factor-II regulates PTEN expression in the mammary gland. J Biol Chem. 2003; 278:50422–50427. [PubMed: 14517213]
35. Vinciguerra M, Carrozzino F, Peyrou M, Carlone S, Montesano R, Benelli R, et al. Unsaturated fatty acids promote hepatoma proliferation and progression through downregulation of the tumor suppressor PTEN. J Hepatol. 2009; 50:1132–1141. [PubMed: 19398230]
36. Oerlemans R, Vink J, Dijkmans BAC, Assaraf YG, van Miltenburg M, van der Heijden J, et al. Sulfasalazine sensitises human monocytic/macrophage cells for glucocorticoids by upregulation of glucocorticoid receptor and glucocorticoid induced apoptosis. Ann Rheum Dis. 2007; 66:1289–1295. [PubMed: 17267514]

37. Charalambous MP, Lightfoot T, Speirs V, Horgan K, Gooderham NJ. Expression of COX-2, NF-kappaB-p65, NF-kappaB-p50 and IKKalpha in malignant and adjacent normal human colorectal tissue. Br J Cancer. 2009; 101:106–115. [PubMed: 19513071]
38. Visconti R, Cerutti J, Battista S, Fedele M, Trapasso F, Zeki K, et al. Expression of the neoplastic phenotype by human thyroid carcinoma cell lines requires NFkappaB p65 protein expression. Oncogene. 1997; 15:1987–1994. [PubMed: 9365245]
39. Gu L, Findley HW, Zhou M. MDM2 induces NF-kappaB/p65 expression transcriptionally through Sp1-binding sites: a novel, p53-independent role of MDM2 in doxorubicin resistance in acute lymphoblastic leukemia. Blood. 2002; 99:3367–3375. [PubMed: 11964305]
40. Ahmed KM, Nantajit D, Fan M, Murley JS, Grdina DJ, Li JJ. Coactivation of ATM/ERK/NF-kappaB in the low-dose radiation-induced radioadaptive response in human skin keratinocytes. Free Radic Biol Med. 2009; 46:1543–1550. [PubMed: 19324081]
41. Leighton PA, Saam JR, Ingram RS, Stewart CL, Tilghman SM. An enhancer deletion affects both H19 and Igf2 expression. Genes Dev. 1995; 9:2079–2089. [PubMed: 7544754]
42. Runge S, Nielsen FC, Nielsen J, Lykke-Andersen J, Wewer UM, Christiansen J. H19 RNA binds four molecules of insulin-like growth factor II mRNA-binding protein. J Biol Chem. 2000; 275:29562–29569. [PubMed: 10875929]
43. Brannan CI, Dees EC, Ingram RS, Tilghman SM. The product of the H19 gene may function as an RNA. Mol Cell Biol. 1990; 10:28–36. [PubMed: 1688465]
44. Reik W, Walter J. Genomic imprinting: parental influence on the genome. Nat Rev Genet. 2001; 2:21–32. [PubMed: 11253064]
45. Ohlsson R, Hedborg F, Holmgren L, Walsh C, Ekstrom TJ. Overlapping patterns of IGF2 and H19 expression during human development: biallelic IGF2 expression correlates with a lack of H19 expression. Development. 1994; 120:361–368. [PubMed: 8149914]
46. Li X, Nong Z, Ekstrom C, Larsson E, Nordlinder H, Hofmann WJ, et al. Disrupted IGF2 promoter control by silencing of promoter P1 in human hepatocellular carcinoma. Cancer Res. 1997; 57:2048–2054. [PubMed: 9158004]
47. Ariel I, Ayesh S, Perlman EJ, Pizov G, Tanos V, Schneider T, et al. The product of the imprinted H19 gene is an oncofetal RNA. Mol Pathol. 1997; 50:34–44. [PubMed: 9208812]
48. Feinberg AP, Vogelstein B. Hypomethylation of ras oncogenes in primary human cancers. Biochem Biophys Res Commun. 1983; 111:47–54. [PubMed: 6187346]
49. Halonen M, Pelto-Huikko M, Eskelin P, Peltonen L, Ulmanen I, Kolmer M. Subcellular Location and Expression Pattern of Autoimmune Regulator (Aire), the Mouse Orthologue for Human Gene Defective in Autoimmune Polyendocrinopathy Candidiasis Ectodermal Dystrophy. J Histochem Cytochem. 2001; 49:197–208. [PubMed: 11156688]

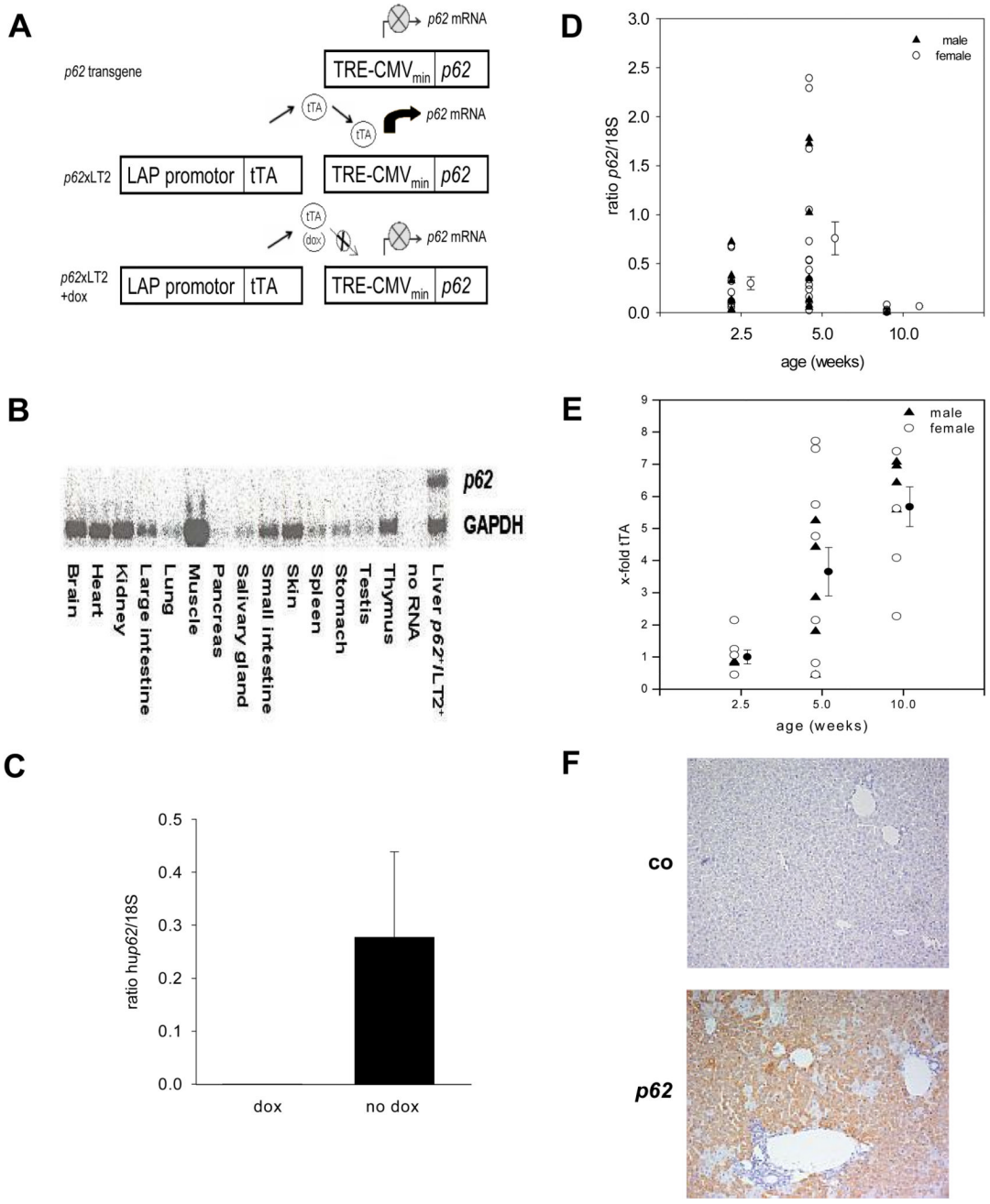

Fig. 1. Hepatic *p62* overexpression

(A) Generation of *p62* transgenic mice. No expression of *p62* mRNA under TRE-CMV promotor control (upper panel). Liver-specific expression of *p62* mRNA in double-positive $p62^{+}$/$LT2^{+}$ mice (middle panel). Application of doxycycline inhibits transgene expression (lower panel). $TRE\text{-}CMV_{min}$: transrepressor responsive element cytomegalovirus; tTA: tetracycline transactivator; LAP: liver enriched activator protein; dox: doxycycline (B) *p62* expression in different mouse organs. The Northern Blot detects the 2.0 kb band of *p62* mRNA only in livers of *p62* transgenic mice. (C) *p62* mRNA expression after doxycycline (dox) administration. (D) Hepatic *p62* mRNA expression (n=14/2.5 weeks, n=21/5 weeks,

and n=8/10 weeks). (E) tTA expression in $LT2^{+}$ mice (n=7/2.5 weeks, 12/5 weeks, and 8/10 weeks). (F) *p62* immunohistochemistry.

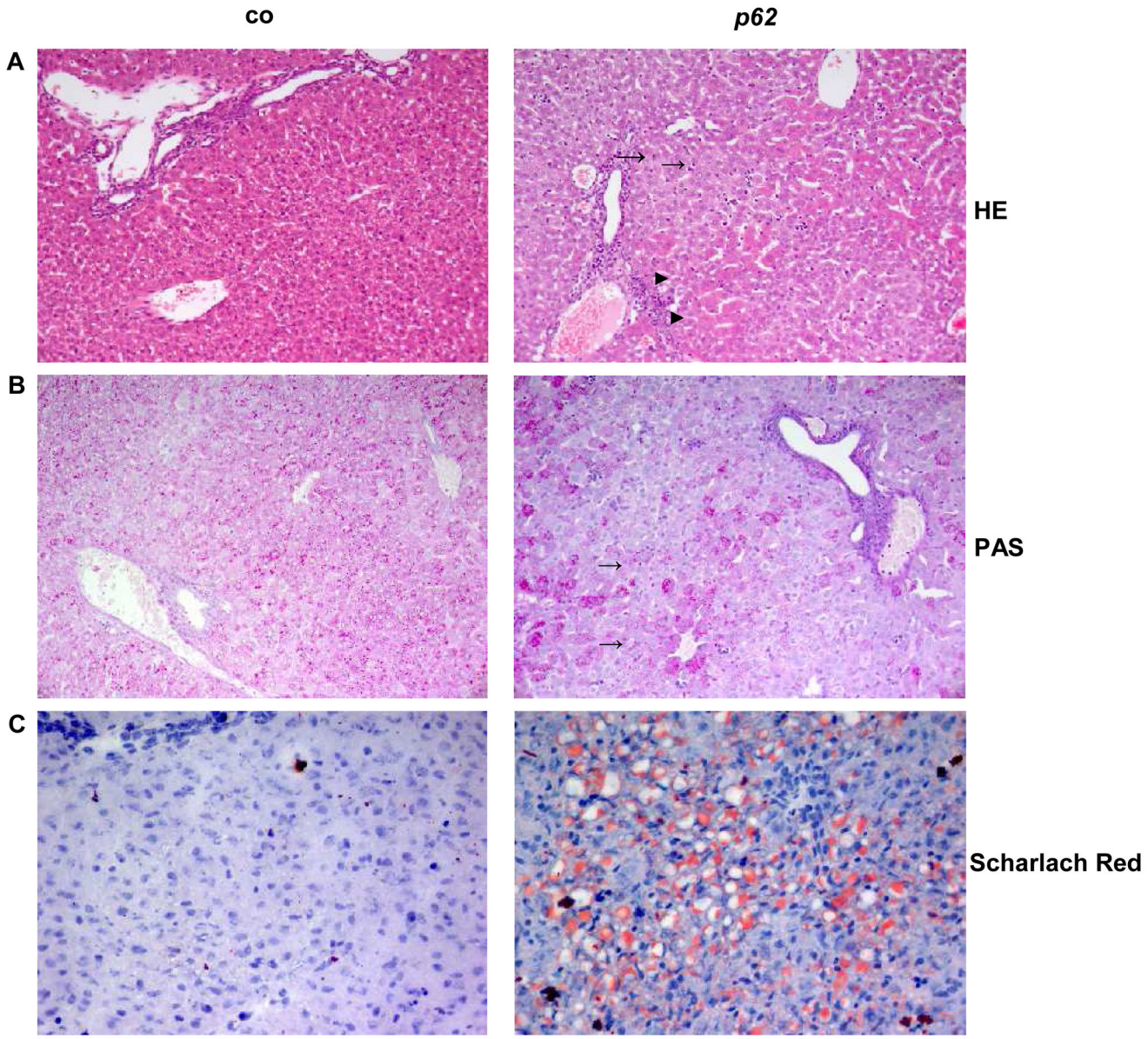

Fig. 2. Liver histology of 2.5 week old animals

(A) HE-stained liver tissue. Pericentrally located basophilic cells (→) were only detected in *p62* transgenic animals. (►) displays eosinophilic cells. (B) Glycogen staining. (→) show the accumulation of glycogen around the central vein. (C) Scharlach Red stained cryosections. A microvesicular distribution of fatty acids occurred in hepatocytes of transgenic animals. (co, n=11, *p62*, n=21). (A/B: 20×, C: 40× original magnification)

animals (age)		body weight (g)	liver weight (g)	liver to body weight ratio
co	2.5 weeks	8.62 ± 0.19	0.33 ± 0.01	3.85 ± 0.06
	5 weeks	15.73 ± 0.70	0.79 ± 0.06	4.95 ± 0.19
	10 weeks	22.42 ± 1.02	1.31 ± 0.30	5.78 ± 0.21
p62	2.5 weeks	8.23 ± 0.19	0.33 ± 0.01	**4.08 ± 0.07 (*p<.05)**
	5 weeks	15.32 ± 0.37	0.75 ± 0.14	4.89 ± 0.16
	10 weeks	22.71 ± 1.40	1.28 ± 0.29	5.58 ± 0.28

		ALT	AST	*De Ritis* ratio	HDLC	CHOL	TG
co	both sexes	583± 177	2564 ± 280	6.29 ± 0.62	86 ± 3	102 ± 6	111 ± 12
	male	312± 36	2289 ± 189	7.72 ± 0.58	89 ± 4	108 ± 9	85 ± 13
	female	932 ± 375	2918 ± 592	4.45 ± 0.78	84 ± 5	93 ± 5	144 ± 15
p62	both sexes	354 ± 69	1749 ± 244 (*p<0.05)	5.99 ± 0.87	89 ± 6	103 ± 7	116 ± 13
	male	425 ± 94	1798 ± 236	5.45 ± 1.36	90 ± 9	102 ±11	109 ± 8
	female	248 ± 87	1677 ± 552	6.81 ± 0.88	86 ± 5	105 ± 4	125 ± 31

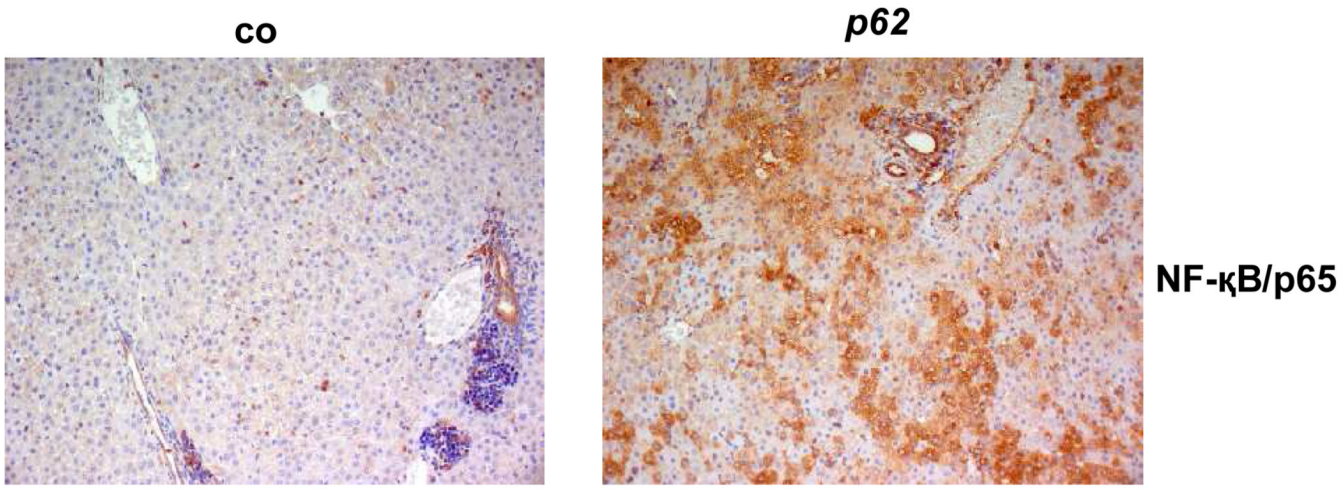

Fig. 3. Fatty liver and serum parameters

(A) Weight parameters of 2.5 (n=co:26/*p62*: 29), 5 (n=co: 12/*p62*: 12), and 10 (n=co: 6/*p62*: 3) week old mice. (B) Serum parameters of 2.5 week old *p62* transgenic mice (*p62*: n=10, of

which n=6 male and n=4 female) *vs.* controls (n=16, of which n=9 male and n=7 female). Lipids expressed in mg/dl, transaminases expressed in U/l. (C) Immunostaining of the NF-κB subunit p65 (left: co, n=7, right: *p62*, n=15).

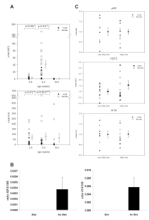

Fig. 4. H19 and *Igf2* expression

(A) Time course of *Igf2* and *H19* mRNA expression (n=14/2.5 weeks, 21/5 weeks, 8/10 weeks). (B) *Igf2* and *H19* mRNA expression after doxycyclin (dox) administration. (C) *p62*, *Igf2* and *H19* mRNA expression in non-fatty transgenic (n=8) *vs.* fatty transgenic livers (n=11) with values for non-fatty transgenic livers set as 1.

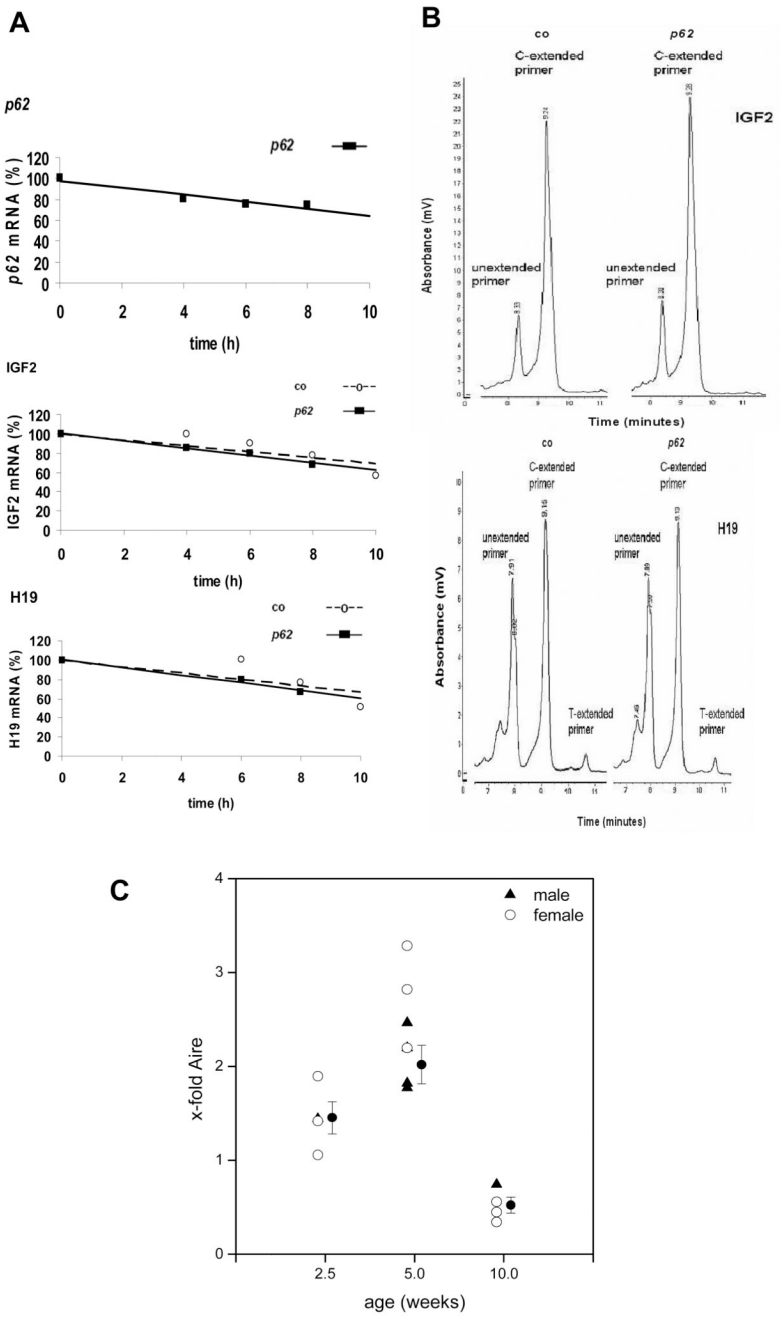

Fig. 5. Mechanism of *Igf2* and *H19* induction

(A) mRNA stability in *p62* transgenic (n=3) *vs.* control (n=3) hepatocytes, expressed relative to t=0 h. (B) Allele-specific expression of *Igf2* and *H19*. Representative HPLC chromatogram showing amplification products for *Igf2* (above) and *H19* (below). (C) Time course of Aire mRNA expression (n=4 at 2.5 weeks, 7 at 5 weeks and 4 at 10 weeks).

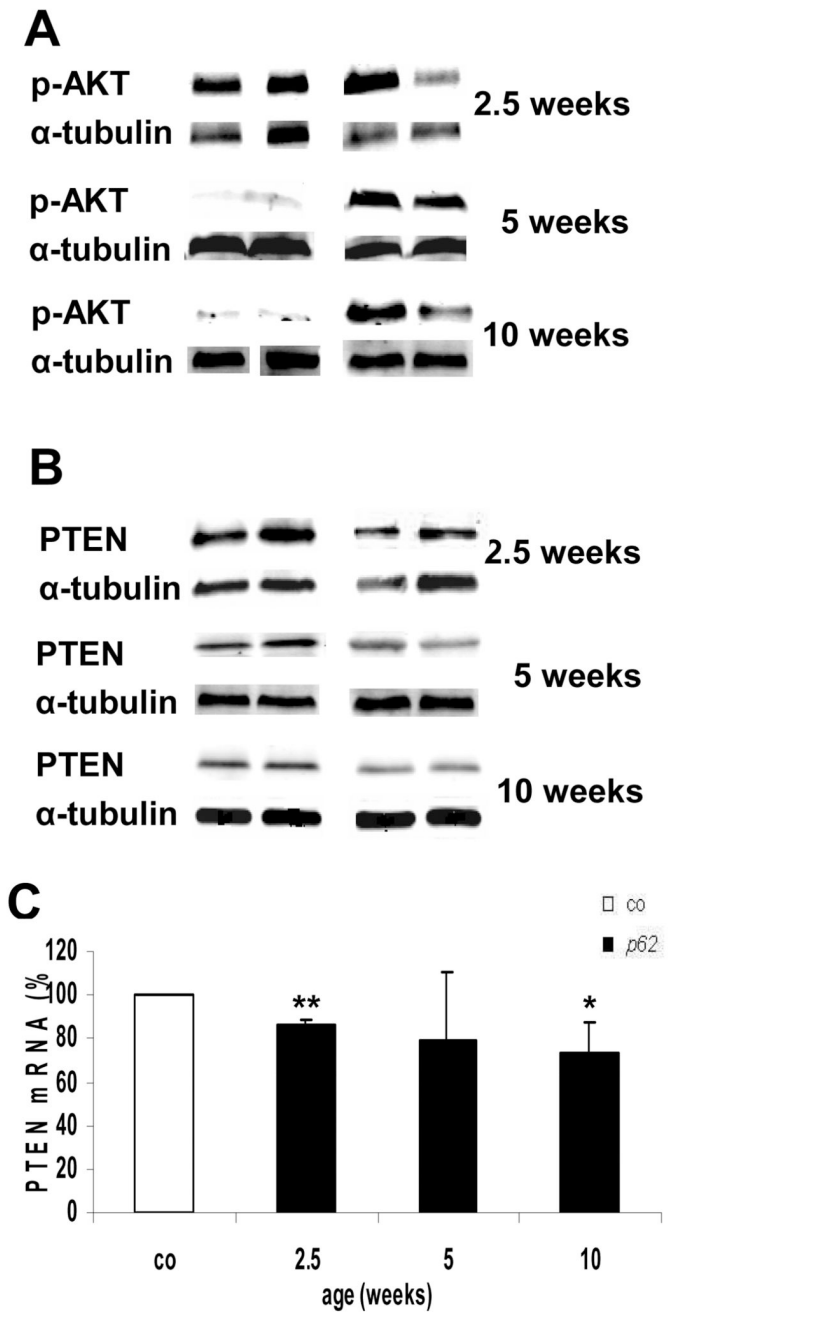

Fig. 6. *Igf2* downstream target activation

(A) pAKT and (B) PTEN at 2.5 (n=co:6/*p62*: 7), 5 (n=co: 4/*p62*: 5) and 10 weeks (n=co: 7/*p62*: 6). Protein normalized to α-tubulin. Representative blots are shown. (C) PTEN mRNA expression of 2.5 (n=co:8/*p62*: 13), 5 (n=co: 4/*p62*: 6) and 10 week (n=co: 8/*p62*: 12), mean percentages ± SEMs are shown. P<.01 (**) *vs.* controls of the respective age.

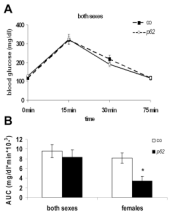

Fig. 7. Glucose tolerance test

(A) Blood glucose values (mg/dl) (co: n=17, *p62*: n=11). (B) AUC (area under the curve) of glucose levels. Values integrated over 75 min *vs.* gender-specific controls.